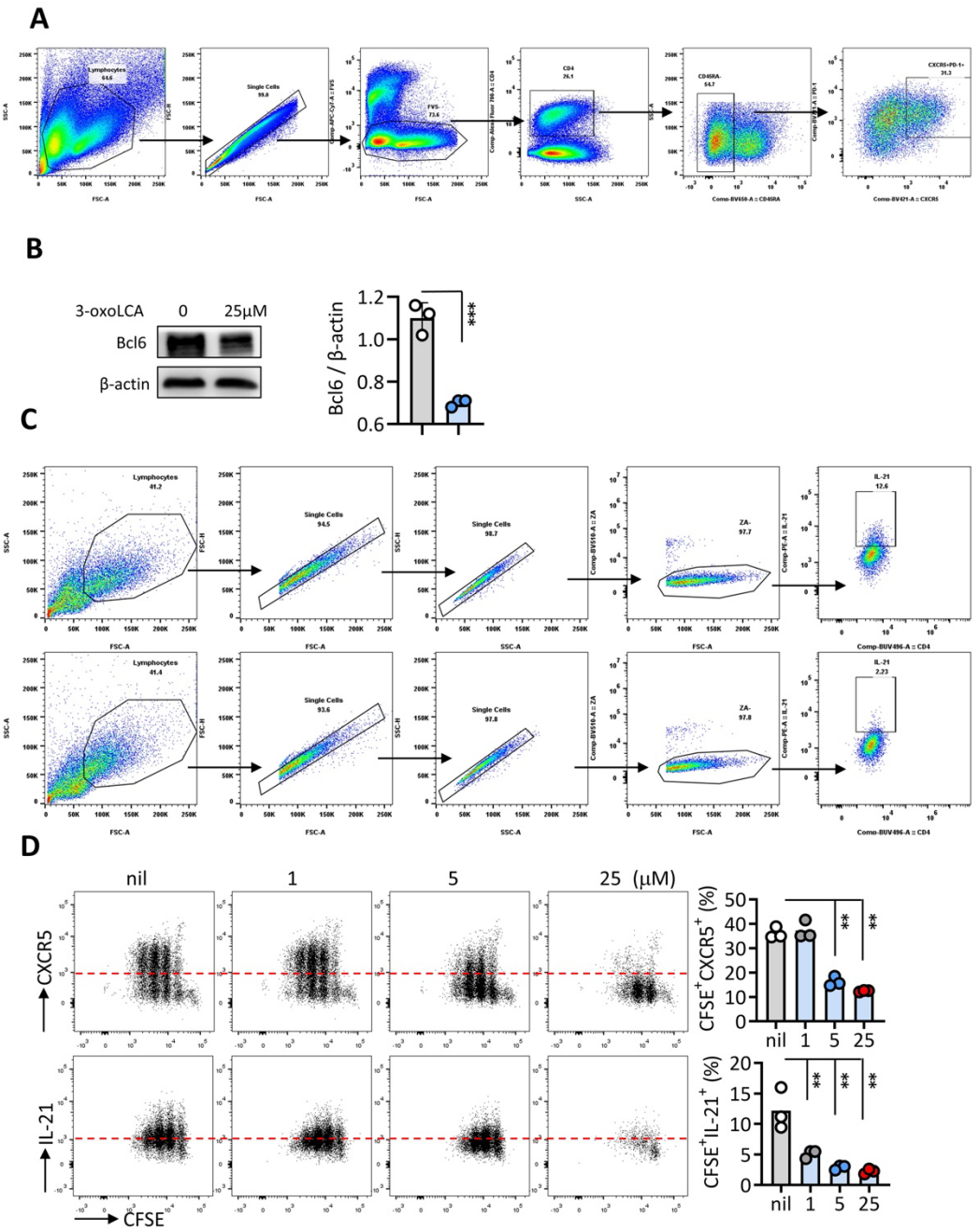

Figure S1. 3-oxoLCA affect Tfh cells differentiation in human CD4$^+$ T cells.

A. The gating strategy to analyse Tfh cell subsets in cultured human CD4$^+$ T cells.

B. Bcl6 expression in WT mouse naive CD4$^+$ T cells stimulated with 3-oxoLCA by Western blot (n=3).

C. The gating strategy to analyse IL-21 positive cells in cultured human CD4$^+$ T cells.

D. The proliferation of cultured human CFSE$^+$CXCR5$^+$ and CFSE$^+$IL21$^+$ T cells by CFSE assay (n=3).

The graphs show the data as mean ± SEM. *$p < 0.05$, **$p < 0.01$, ***$p < 0.001$, ****$p < 0.0001$.

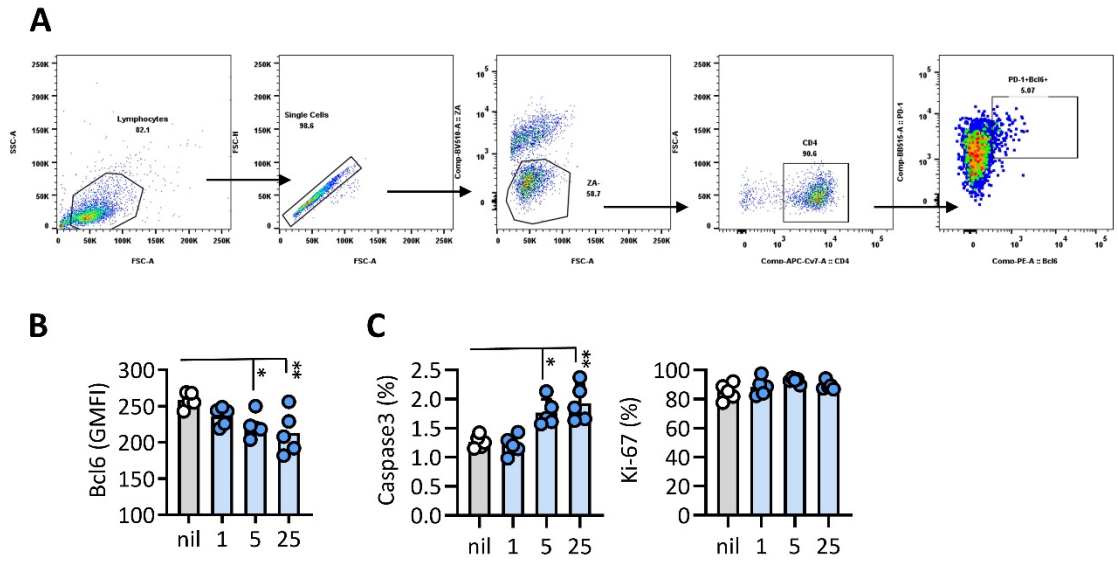

Figure S2. 3-oxoLCA affect Tfh cells differentiation in mouse CD4$^+$ T cells.

A. The gating strategy to analyse Tfh cell subsets in cultured mouse CD4$^+$ T cells.

B. The geometric mean fluorescence intensity (GMFI) of Bcl6 expression at different concentrations of 3-oxoLCA (n=5).

C. The percentage of Caspase-3 and Ki-67 of CD4$^+$ T cells at different concentrations of 3-oxoLCA (n=5).

The graphs show the data as mean ± SEM. *$p < 0.05$, **$p < 0.01$, ***$p < 0.001$, ****$p < 0.0001$.

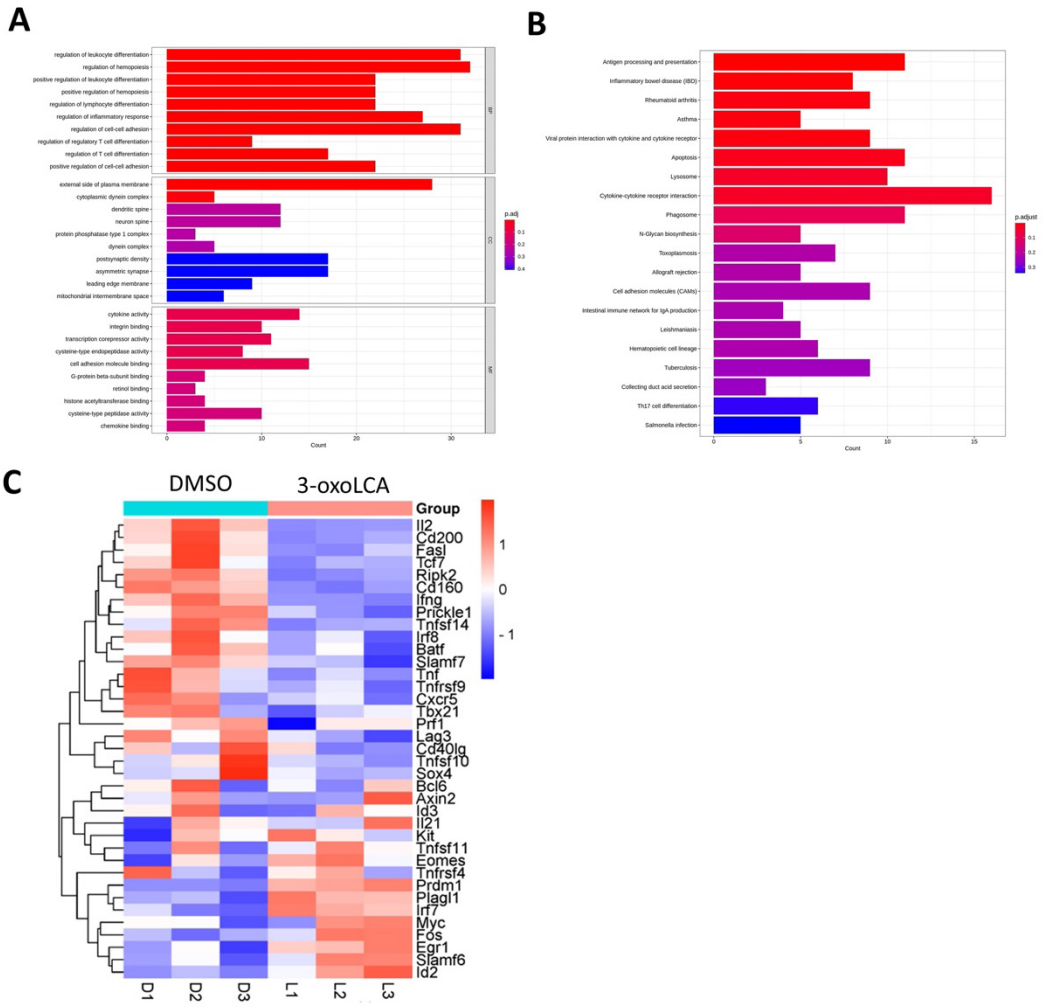

Figure S3. 3-oxoLCA inhibit Tfh cells through improve mitophagy.

A. Gene ontology enrichment analysis was performed on the DEGs that were differentially regulated by either 3-oxoLCA resulted in changes in the expression of genes involved in several biological processes.

B. Top enriched pathways of DEGs in 3-oxoLCA treated Tfh cells by Kyoto Encyclopedia of Genes and Genomes (KEGG) analysis.

C. Heatmap showing the RNA-seq analysis of Tfh-related genes in mouse naïve $CD4^+$ T cells with anti-CD3/CD28 activation for 12h, and further treated with 3-oxoLCA or DMSO for 12 h.

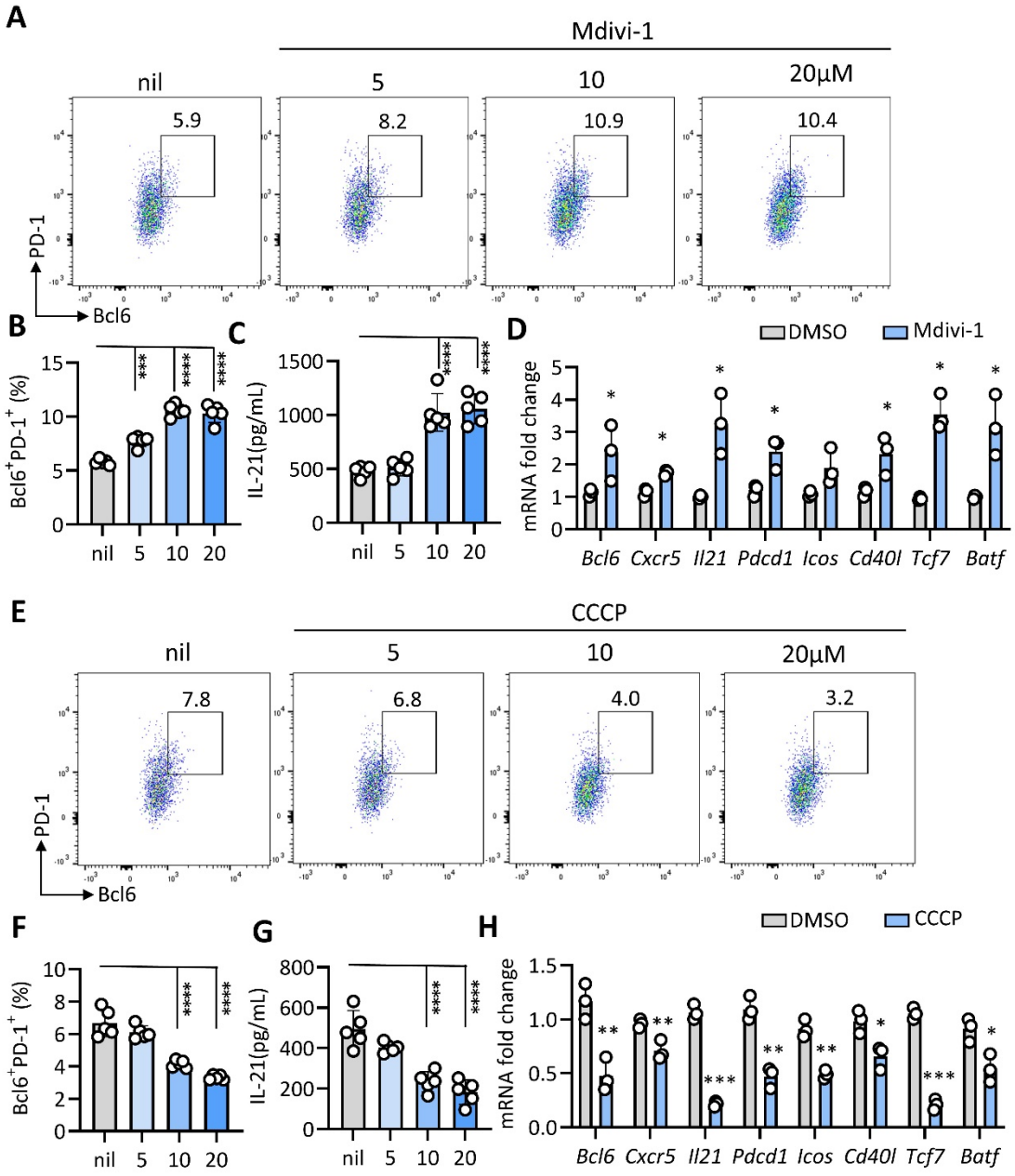

Figure S4. Modulation of intercellular mitophagy regulates Tfh cells differentiation.

A-B. Analysis of PD-1$^+$Bcl6$^+$ Tfh cells in cultured naïve CD4$^+$ T cells from WT mice with mitophagy inhibitor (Mdivi-1) for 3days (n=5).

C. ELISA analysis of IL-21 production in naïve CD4$^+$ T cells from WT mice with Mdivi-1 for 3days (n=5).

D. Tfh-related genes in naïve CD4$^+$ T cells from WT mice treated with Mdivi-1 for 12h by real-time PCR (n=3).

E-F. Analysis of PD-1$^+$Bcl6$^+$ Tfh cells in cultured naïve CD4$^+$ T cells from WT mice with mitophagy inducer (CCCP) for 3days (n=5).

G. ELISA analysis of IL-21 production in naïve CD4$^+$ T cells from WT mice with mitophagy inducer (CCCP) for 3days (n=5).

H. Tfh-related genes in naïve CD4$^+$ T cells from WT mice treated with CCCP for 12h by real-time PCR (n=5).

The graphs show the data as mean ± SEM. *$p < 0.05$, **$p < 0.01$, ***$p < 0.001$, ****$p < 0.0001$.

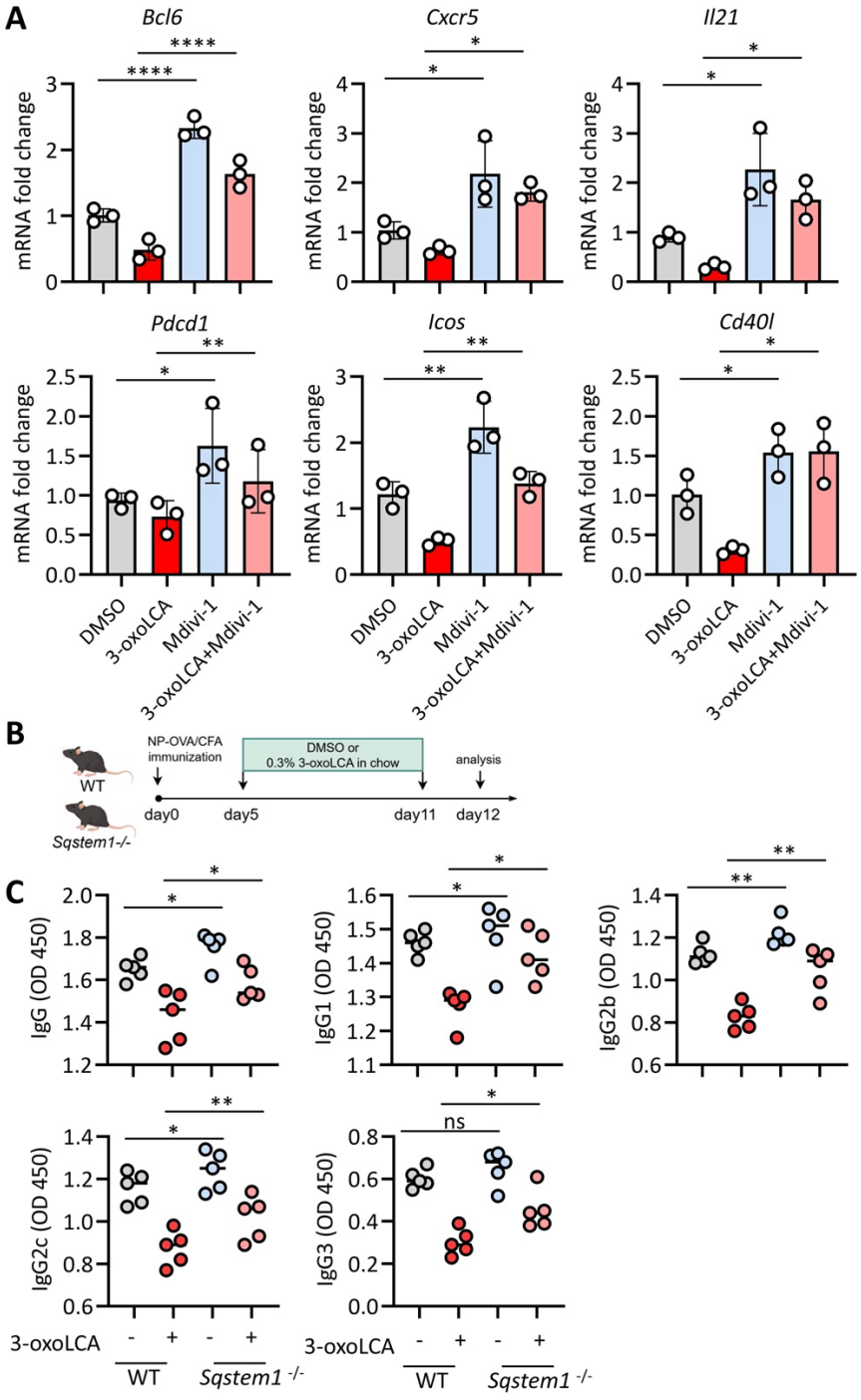

Figure S5. Inhibition of mitophagy restores 3-oxoLCA induced Tfh cells differentiation deficiency.

A. Real-time quantitative PCR analysis of mRNA abundance of Tfh cell-related genes in DMSO, 3-oxoLCA, Mdivi-1 and 3-oxoLCA + Mdivi-1 group (n=3).

B. Workflow of the experimental procedure of WT or *Sqstem1*$^{-/-}$ C57BL/6 mice with NP-OVA/CFA immunization (subcutaneous), 3-oxoLCA (oral gavage) and analysis.

C.ELISA assay for serum NP-specific IgG1, IgG2b, IgG2c and IgG3 titers from in WT or *Sqstem1*$^{-/-}$ C57BL/6 mice immunized with NP-OVA/CFA, followed by 3-oxoLCA treatment (n=5).

The graphs show the data as mean ± SEM. *$p < 0.05$, **$p < 0.01$, ***$p < 0.001$, ****$p < 0.0001$.

Figure S6. 3-oxoLCA3-oxoLCA reduces Tfh cells blasting associated with attenuated mTORC1 and STAT3 signaling pathway.

The phosphorylation of key signaling proteins (mTOR, p70S6K, S6, STAT3) in WT naïve $CD4^+$ T cells was compared by Western blot following treatment with vehicle control or 25 μM 3-oxoLCA (n=3).

The graphs show the data as mean ± SEM. *$p < 0.05$, **$p < 0.01$, ***$p < 0.001$, ****$p < 0.0001$.

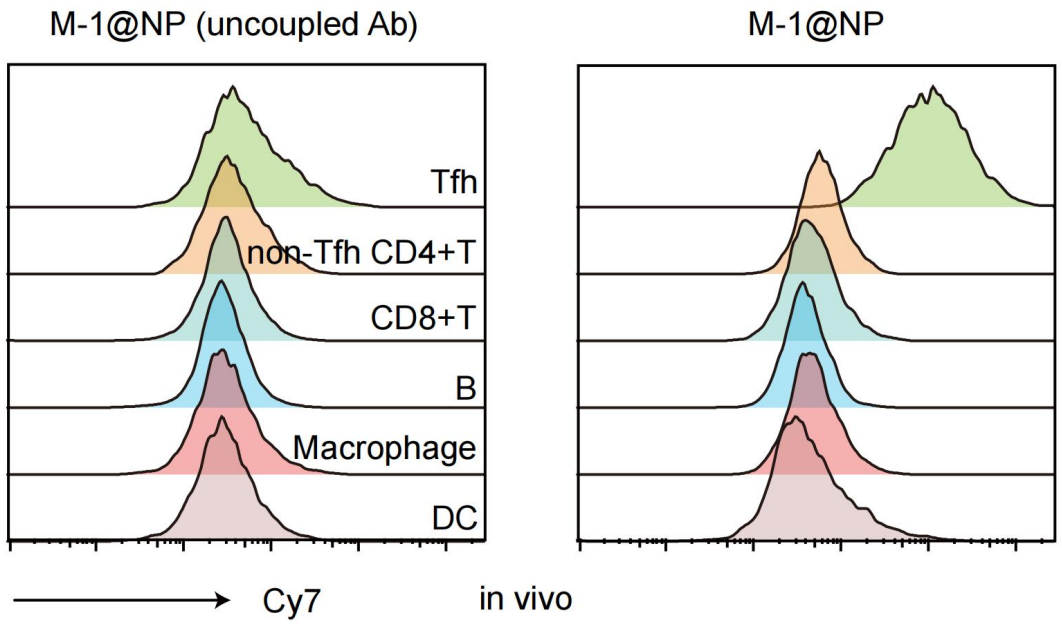

Figure S7. The distribution of M-1@NP in different lymphocyte subsets in vivo by flow cytometry.

The histogram of flow cytometry showing fluorescence intensity of M-1@NP in different immune cell subpopulations in mouse spleen.

The graphs show the data as mean ± SEM. *$p < 0.05$, **$p < 0.01$, ***$p < 0.001$, ****$p < 0.0001$.

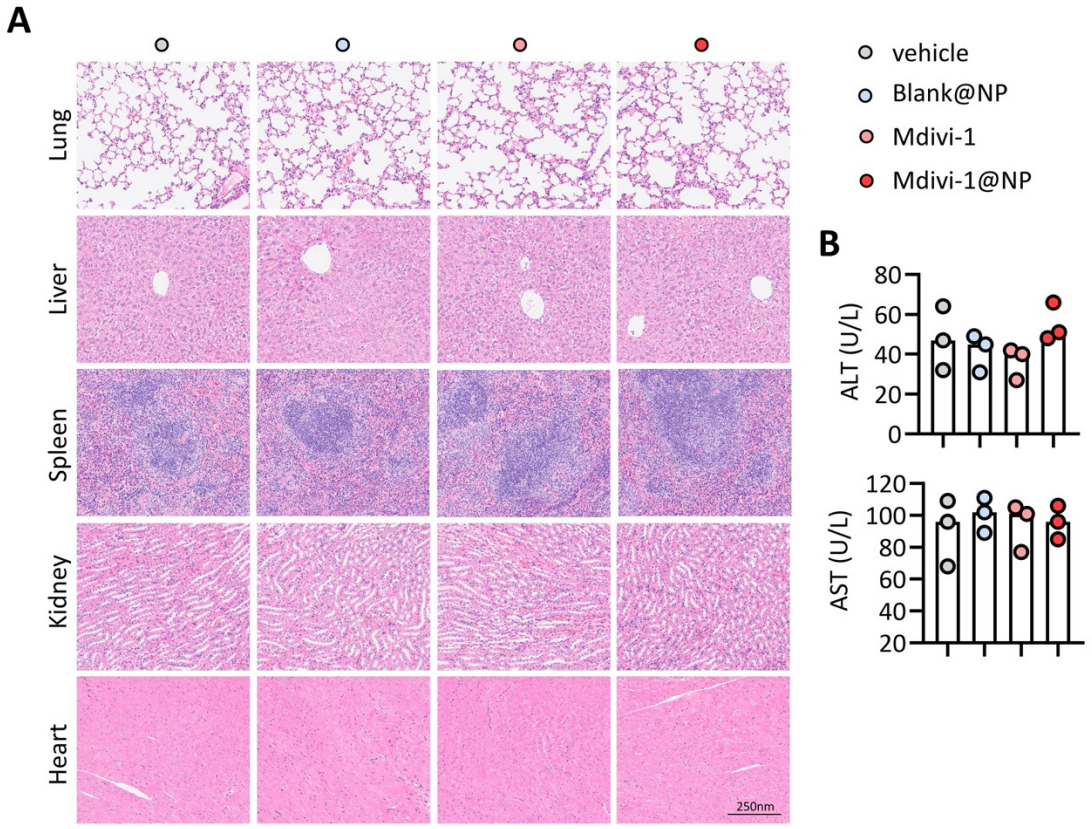

Figure S8. In vivo biocompatibility assessment.

A. Major organs of mice were taken for H&E staining at time points of 12 days after M-1@NP injection.

B. Serum glutathione transaminase and ghrelin levels in mice injected with the M-1@NP in the tail vein after 12 days (n = 3).

The graphs show the data as mean ± SEM. *$p < 0.05$, **$p < 0.01$, ***$p < 0.001$, ****$p < 0.0001$.

Supplementary Table S1. PCR primers of mouse used in this study

genes	Forward Sequence	Reverse Sequence
Bcl6	CAGAGATGTGCCTCCATACTGC	CTCCTCAGAGAAACGGCAGTCA
Cxcr5	ATCGTCCATGCTGTTCACGCCT	CAACCTTGGCAAAGAGGAGTTCC
Il21	GCCTCCTGATTAGACTTCGTCAC	CAGGCAAAAGCTGCATGCTCAC
Pdcd1	CGGTTTCAAGGCATGGTCATTGG	TCAGAGTGTCGTCCTTGCTTCC
Icos	GCAGCTTTCGTTGTGGTACTCC	TGTGTTGACTGCCGCCATGAAC
Cd40l	GAACTGTGAGGAGATGAGAAGGC	TGGCTTCGCTTACAACGTGTGC
Tcf7	CCTGCGGATATAGACAGCACTTC	TGTCCAGGTACACCAGATCCCA
Batf	CACAGAAAGCCGACACCCTTCA	GCTGCTCAGCACTGATGTGAAG
Atg5	CTTGCATCAAGTTCAGCTCTTCC	AAGTGAGCCTCAACCGCATCCT
Atg7	CCTGTGAGCTTGGATCAAAGGC	GAGCAAGGAGACCAGAACAGTG
Ulk1	GCAGCAAAGACTCCTGTGACAC	CCACTACACAGCAGGCTATCAG
Becn1	CAGCCTCTGAAACTGGACACGA	CTCTCCTGAGTTAGCCTCTTCC
Pink1	CGACAACATCCTTGTGGAGTGG	CATTGCCACCACGCTCTACACT
Bnip3	GCTCCAAGAGTTCTCACTGTGAC	GTTTTTCTCGCCAAAGCTGTGGC
Fundc1	AGACACCACTGGTGGAATCGAG	CCTTCTGGAATAAAAATCCTGCAC

Supplementary Table S2. PCR primers of human used in this study.

genes	Forward Sequence	Reverse Sequence
BCL6	CATGCAGAGATGTGCCTCCACA	TCAGAGAAGCGGCAGTCACACT
CXCR5	TGAAGTTCCGCAGTGACCTGTC	GAGGTGGCATTCTCTGACTCAG
IL21	CCAAGGTCAAGATCGCCACATG	TGGAGCTGGCAGAAATTCAGGG
PDCD1	AAGGCGCAGATCAAAGAGAGCC	CAACCACCAGGGTTTGGAACTG
ICOS	CCCATAGGATGTGCAGCCTTTG	GGCTGTGTTCACTGCTCTCATG
CD40L	GCGGCACATGTCATAAGTGAGG	GTCCTTGTCTTTTAACGGTCAGC